Pis'ma v ZhETF, vol. 87, iss. 6, pp. 362 – 366 © 2008 March 25

Enhanced super-hyperfine structure of EPR spectra of U^{3+} ion in the Van Vleck paramagnet $LiTmF_4$

L. K. Aminov, A. A. Ershova, S. L. Korableva, I. N. Kurkin, A. A. Rodionov, B. Z. Malkin[1)]

Kazan State University, 420008 Kazan, Russia

Submitted 11 February 2008

The observation of the super-hyperfine structure (SHFS) of EPR spectra due to enhanced nuclear magnetism is reported. The X-band spectrum of U^{3+} ion introduced into the Van Vleck paramagnet $LiTmF_4$ was measured in the temperature range of 5–20 K and compared with the spectra of $LiLuF_4$:U^{3+} and $LiYF_4$:U^{3+} single crystals. The spectra reveal well resolved and strikingly different SHFS. SHFS of Li(Lu,Y)F_4:U^{3+} is due to fluorine ions forming the nearest surroundings of the U^{3+} ion. The main contribution to SHFS of the U^{3+} spectrum in $LiTmF_4$ is coming from Tm^{3+} ions with highly enhanced nuclear gyromagnetic tensor.

PACS: 75.10.Dg, 75.30.Et, 76.30.Kg

Recently we have measured EPR spectra in the $LiLuF_4$:U single crystal; the observed EPR signals were unambiguously assigned to the U^{3+} ions [1]. The pronounced SHFS of the spectra has been revealed which is evidently due to the super-hyperfine interaction between the 5f electrons and nuclear magnetic moments of the nearest ligands, that is, eight fluorine ions of the first and second coordination spheres. To obtain more details of the coupling of 5f electrons with ligands, it is interesting to investigate EPR spectra of U^{3+} ion in other double fluorides, and in this letter we present the results of EPR investigations of the $LiTmF_4$:U and $LiYF_4$:U single crystals.

The tetragonal $LiTmF_4$ crystal is especially interesting since it is a typical Van Vleck paramagnet [2]. The ground multiplet $^3H_6$ of the Tm^{3+} ion is split by a crystal field in such a manner that the ground state is a singlet Γ_2 (energy levels are labeled according to the corresponding irreducible representations of the point symmetry group S_4). The first excited level is a doublet $\Gamma_{3,4}$, separated from the ground level by $31\,cm^{-1}$ and coupled to it by transverse magnetic field (B_x,B_y; $z||c$-axis of the crystal), while the nearest singlet level Γ_2, coupled to the ground one by longitudinal field ($B_z = B$), has an energy of $282\,cm^{-1}$. The ^{169}Tm isotope with a nuclear spin $I = 1/2$ has a 100% abundance, the nuclear magnetism being essentially enhanced due to hyperfine interaction. The effective gyromagnetic ratio becomes highly anisotropic tensor with $\gamma_{||} = (1 + \alpha_{||})\gamma_I = 2.73\gamma_I$ and $\gamma_\perp = (1 + \alpha_\perp)\gamma_I = 67.5\gamma_I$, where $\gamma_I/2\pi = -3.540\,MHz/T$ for the Tm nucleus [2]. One can propose that due to such large magnetic moment the super-hyperfine interaction of a doped paramagnetic ion with thulium nuclei disposed in an undistorted crystal at a distance of $R_3 \approx 0.37\,nm$ is not less than with fluorine nuclei disposed at distances $R_1 \approx 0.222$ and $R_2 \approx 0.227\,nm$. Indeed, the appearance of the EPR spectra of U^{3+} ion in $LiTmF_4$ occurs to be strikingly different from that in isomorphic crystals $LiLuF_4$ (see Fig.1) and $LiYF_4$.

EPR spectra were taken with Bruker ESP-300 spectrometer at the frequency of $\approx 9.4\,GHz$ (X-band) and at temperatures in the range of 5–20 K. The samples were grown by Bridgman-Stockbarger method, in the argon atmosphere. The uranium was admixed to the crystal in the form of UF_3 compound. The introduction of uranium didn't change the characteristic light green color of $LiTmF_4$ crystal.

Intensive EPR spectra due to U^{3+} ions in $LiTmF_4$:U have been observed which have an axial symmetry and are described by g-factors: $g_{||} = 1.213$, $g_\perp = 2.659$. The spectra for two temperatures, $T = 6$ and 13 K, at $\mathbf{B}||c$ are given in Fig.1. These spectra are due to even isotope ^{238}U with natural abundance 99.28%. Much less intensive spectra with clearly pronounced hyperfine structure due to odd isotope ^{235}U were observed in $LiLuF_4$:U^{3+} [1]. For a comparison, the EPR spectrum in $LiLuF_4$:U^{3+} for even isotope ^{238}U is presented in Fig.1a. The g-factors are close to those in the $LiTmF_4$:U^{3+} crystal: $g_{||} = 1.228$, $g_\perp = 2.516$, however the spectrum in the diamagnetic host matrix doesn't depend on temperature in the considered temperature interval. Our measurements in $LiYF_4$:U^{3+} single crystal showed the spectrum analogous to that given in Fig.1a with $g_{||} = 1.150$ ($g_\perp = 2.508$).

[1)] e-mail: boris.malkin@ksu.ru

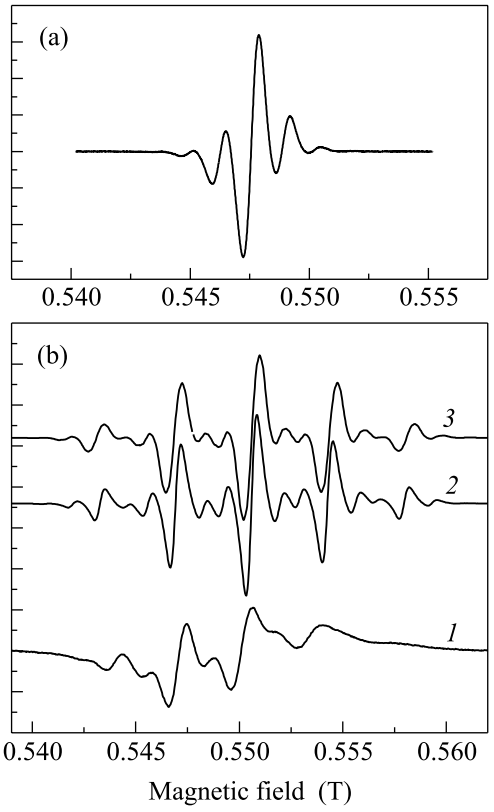

Fig.1. EPR signals in $LiLuF_4$:$^{238}U^{3+}$ ((a), $\nu = 9.42$ GHz, $T = 10$ K) and $LiTmF_4$:U^{3+} ((b), $\nu = 9.35$ GHz) at temperatures 13 (curve *1*) and 6 K (curve *2*) in the magnetic fields parallel to the c-axis. The simulated spectrum is represented by the curve *3*

The complex structure of the observed EPR spectra is evidently due to the super-hyperfine interaction of unfilled $5f$-electron shell with nuclear magnetic moments of ligands. The nearest ligands are eight fluorine ions (see Fig.2), and the super-hyperfine interaction with

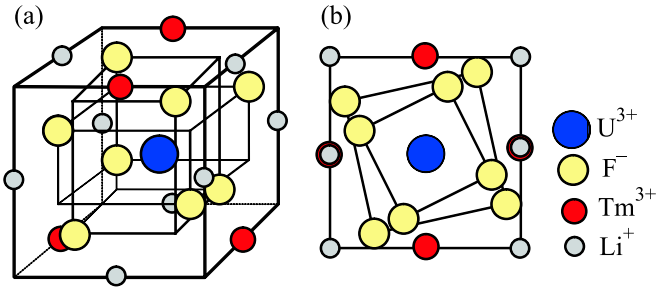

Fig.2. A half of the Bravais cell of $LiTmF_4$ crystal centered in the Tm^{3+} position occupied by the impurity U^{3+} ion (a); a projection of the cell on the ab-plane (b) (not to scale)

their nuclear moments is responsible for the structure of the spectrum in Fig.1a [1]. The sharp difference of the spectra in $LiTmF_4$:U^{3+} from those in $LiLuF_4$:U^{3+} and $LiYF_4$:U^{3+} is most probably explained by that the $LiTmF_4$ compound is a Van Vleck paramagnet, and the magnetic moments of thulium nuclei are strongly enhanced. So an interaction of $5f$-electrons with thulium nuclei may be of the same order of magnitude as interaction with fluorine nuclei. More detailed discussion is given below.

The U^{3+} ions substitute for R^{3+} ions in double fluorides $LiRF_4$ (R=Y, Lu, Tm) in the sites with S_4 point symmetry. The nearest surrounding of doped ions is constituted by two fours of fluorine ions (the first two coordination spheres, see Fig.2), which form two tetrahedrons, oblate and elongated along the crystallographic c-axis ($z||c$), turned around the $c-$axis so that their second-order axes (x, y) do not coincide. The nearest to the impurity U^{3+} ion four R^{3+} ions are forming the fourth coordination sphere. With yet Li^+ ions of the third and fifth coordination spheres one comes to a half of the Bravais cell (shown in Fig.2a) containing two molecules $Li(Tm,U)F_4$. Positions of F^- ions in each group of four are crystallographic equivalent, and for parallel orientation of an applied field, $\mathbf{B}||c$, they are also magnetically equivalent. The same is true for Tm^{3+} ions. Radius vectors coordinating the U^{3+} ion (origin) with fluorine ions of the first and second coordination spheres and thulium ions will be designated as $\mathbf{R}_1$, $\mathbf{R}_2$, and $\mathbf{R}_3$, respectively.

The ground multiplet $^4I_{9/2}$ of the U^{3+} ion in $LiRF_4$:U^{3+} crystals is split by the tetragonal crystal field so that the lowest Kramers doublet is separated from excited doublets by the significant interval exceeding 200 cm^{-1} [3, 4]. Therefore, when analyzing EPR spectra of these ions, it is possible to neglect mixing of different doublets by an applied magnetic field and to consider only the subspace of the ground doublet states $|\alpha\rangle$ and $|\beta\rangle = \theta|\alpha\rangle$ connected by the time reversal operator θ. The basis states are considered as eigenstates of an "effective spin" operator S_z ($S = 1/2$, $S_z|\alpha\rangle = 1/2|\alpha\rangle$, $S_z|\beta\rangle = -1/2|\beta\rangle$), then an arbitrary electronic operator $\widehat{O}$ referring to the ion is projected to the spin subspace as follows:

$$\widehat{O} = 2\langle\alpha|\widehat{O}|\alpha\rangle\widehat{S}_z + \langle\alpha|\widehat{O}|\beta\rangle\widehat{S}_+ + \langle\beta|\widehat{O}|\alpha\rangle\widehat{S}_-. \qquad (1)$$

Let us consider the paramagnetic center ($^{238}U^{3+}$) with the total angular moment $\boldsymbol{J}$ and its ligands (F^- and Tm^{3+} ions) in the magnetic field $\mathbf{B}$, the interaction between ligands is neglected as usual [5, 6]. The Hamiltonian of the system includes the electronic Zee-

man term, the nuclear Zeeman terms, the interaction of $5f$ electrons with the fluorine and thulium nuclear spins:

$$H = g_J \mu_B \mathbf{BJ} + \hbar \sum_i (-\mathbf{B} + \mathbf{N}^{(i)}) \tilde{\gamma}^{(i)} \mathbf{I}^{(i)}, \qquad (2)$$

here g_J is the Lande factor and μ_B is the Bohr magneton, the sum is over ligands (eight fluorine and four thulium nuclei), $\tilde{\gamma}^{(i)}$ is the effective nuclear gyromagnetic factor for the i-th ligand. The vector $\mathbf{N}^{(i)}$ is given in the general form in terms of one-electron operators in [5]. The Hamiltonian (2) may be presented in an effective form (1) as follows:

$$\widehat{H}_{\text{eff}} = \sum_{q\nu} g_{q\nu} \mu_B S_\nu B_q + \\ + \hbar \sum_i \left(-\mathbf{B} \tilde{\gamma}^{(i)} \mathbf{I}^{(i)} + \sum_{p\nu} T_{p\nu}^{(i)} (\tilde{\gamma}^{(i)} I^{(i)})_p S_\nu \right), \qquad (3)$$

where $g_{pz} = 2g_J \langle \alpha | J_p | \alpha \rangle$, $T_{pz}^{(i)} = 2\langle \alpha \left| N_p^{(i)} \right| \alpha \rangle$, etc. The SHFS "tensors" $T^{(i)}$ within each four of equivalent ligands are connected by symmetry operations. Within the phenomenological approach three sets of components $T_{p\nu}^{(1)}$), $T_{p\nu}^{(2)}$), and $T_{p\nu}^{(3)}$ for different fours of ligands (F1, F2 and Tm, respectively) are independent parameters of the model.

If the $5f$-electron functions were strictly localized in the nearest vicinity of the origin, the operator $\mathbf{N}^{(i)} \tilde{\gamma}^{(i)} \mathbf{I}^{(i)}$ in eq. (2) could be reduced to the interaction of the point magnetic dipoles, the electronic ($g_J \mu_B \mathbf{J}$) and nuclear ($\tilde{\gamma}^{(i)} \mathbf{I}^{(i)}$) ones disposed at the origin and at a point $\mathbf{R}_i$, respectively. The magnetic dipole-dipole contribution to the parameters $T_{p\nu}^{(i)}$ has the following form:

$$T_{p\nu d}^{(i)} = -\frac{\mu_B}{R_i^3} \sum_q (\delta_{pq} - 3 n_p^i n_q^i) g_{q\nu}, \qquad (4)$$

where $\mathbf{n}^i = \mathbf{R}_i / R_i$. There are also contributions due to small admixture of s-, p-orbitals of the nearest ligands to f-orbitals of the central ion (see [5, 7, 8]) and to exchange interactions between U^{3+} and Tm^{3+} ions.

The electronic Zeeman energy is much greater than other terms in (3), and its diagonalization at $\mathbf{B} || z$ brings to two energy levels $E_\pm = \pm 1/2 g_{||} \mu_B B$ ($g_{||} = g_{zz}$), separated by the interval $g_{||} \mu_B B = \hbar \omega_0$. The corresponding eigenstates $|M_z = \pm 1/2\rangle$ in this case coincide with $|\alpha\rangle$ and $|\beta\rangle$. The nuclear part of the Hamiltonian (3) is diagonalized independently in each electronic state, and in the framework of the admitted approximation of non-interacting ligands, this procedure reduces to diagonalization of individual ligand Hamiltonians $H^{(i)}(M_z)$ at fixed electronic state M_z:

$$H^{(i)}(M_z) = \gamma_I^{(i)} \hbar \mathbf{B}_{\text{eff}}^{(i)}(M_z) \mathbf{I}^{(i)} = \\ = -\gamma_I^{(i)} \hbar \left[(1 + \alpha_{zz}^{(i)}) B I_z^{(i)} - M_z \sum_p (1 + \alpha_{pp}^{(i)}) T_{pz}^{(i)} I_p^{(i)} \right]. \qquad (5)$$

The gyromagnetic ratio is enhanced only for Tm nuclei; in a perfect $LiTmF_4$ crystal the amplification coefficient $(1 + \boldsymbol{\alpha})$ is diagonal in crystallographic axes ($\alpha_{zz} = \alpha_{||}$, $\alpha_{xx} = \alpha_{yy} = \alpha_\perp$). For fluorine ion, $\boldsymbol{\alpha}(F) = 0$. Therefore the problem once again is reduced to diagonalization of the Hamiltonian of the spin $I = 1/2$ in an effective magnetic field (we drop an index i for a while):

$$\mathbf{B}_{\text{eff}}(M_z) = \\ [M_z T_{xz}(1+\alpha_\perp), M_z T_{yz}(1+\alpha_\perp), (M_z T_{zz} - B)(1+\alpha_{||})]. \qquad (6)$$

The energies are as follows:

$$\varepsilon_\pm(M_z) = \pm \frac{1}{2} \gamma_I \hbar B_{\text{eff}}(M_z) = \\ \pm \frac{1}{2} \gamma_I \hbar \sqrt{(M_z T_{zz} - B)^2 (1+\alpha_{||})^2 + M_z^2 T_t^2 (1+\alpha_\perp)^2}, \qquad (7)$$

($T_t^2 = T_{xz}^2 + T_{yz}^2$) and the corresponding eigenstates will be denoted as $|M_z, \pm\rangle$.

The intensity of the electron-nuclear transition between states $|M_z, m\rangle$ and $|-M_z, m'\rangle$ due to the microwave field $\mathbf{B}_1(t) \perp z$ is described by two quantities r, q:

$$r = |\langle M_z, +|\mu_\perp|-M_z, +\rangle|^2 = |\langle M_z, -|\mu_\perp|-M_z, -\rangle|^2 = \\ = \frac{1}{2} A^2 [1 + \mathbf{n}_e(M_z) \mathbf{n}_e(-M_z)], \\ q = |\langle M_z, -|\mu_\perp|-M_z, +\rangle|^2 = |\langle M_z, +|\mu_\perp|-M_z, -\rangle|^2 = \\ = \frac{1}{2} A^2 [1 - \mathbf{n}_e(M_z) \mathbf{n}_e(-M_z)], \qquad (8)$$

where $\mu_\perp$ is the electronic magnetic moment projected on the $\mathbf{B}_1$, $A = \langle M_z | \mu_\perp | - M_z \rangle$ and $\mathbf{n}_e(M_z) = \mathbf{B}_{\text{eff}}(M_z) / B_{\text{eff}}(M_z)$. Note that the value $\mathbf{n}_e(M_z) \cdot \mathbf{n}_e(-M_z)$ is equal to cosine of an angle between the directions of effective magnetic fields on the ligand in two different electronic states.

The diagram of electron-nuclear levels and resonance transitions are shown in Fig.3 for the case of one ligand. The whole energy spectrum is obtained as a result of superposition of such diagrams related to all ligands, so the energy of electron-nuclear state $|M_z, m^{(1)}(M_z), m^{(2)}(M_z), \ldots\rangle$ equals:

$$E(M_z, \{m^{(i)}\}) = M_z g_{||} \mu_B B + \\ + \sum_i m^{(i)}(M_z) \gamma_I^{(i)} \hbar B_{\text{eff}}^{(i)}(M_z). \qquad (9)$$

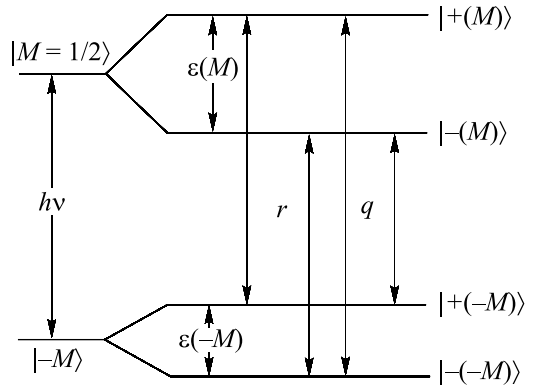

Fig.3. The electron-nuclear energy levels for a paramagnetic center ($S = 1/2$) and one ligand ($I = 1/2$)

Here $m^{(i)}(M_z) = \pm\ 1/2$ for $|M_z, \pm\rangle$ states. For N nonequivalent ligands, the number of sublevels is 2^N in general case, and the spectrum consists of 2^{2N} lines, intensities of these lines are defined as follows:

$$I(|M_z, \{m^{(i)}\}\rangle \leftrightarrow |-M_z, \{m'^{(i)}\}\rangle) = \\ = \prod_i (r^{(i)})^{|m^{(i)}+m'^{(i)}|}(q^{(i)})^{|m^{(i)}-m'^{(i)}|}. \qquad (10)$$

When some ligands are equivalent, the degeneracy of nuclear sublevels arises, and the spectrum is somewhat simplified. For four equivalent ligands the scheme of five equidistant sublevels is obtained with energies

$$E(M_z, I(M_z)) = M_z g_{||}\mu_B B + \gamma_I \hbar I(M_z) B_{\text{eff}}(M_z), \qquad (11)$$

where $I(M_z) = 0, \pm 1, \pm 2$. The multiplet $I(M_z)$ consists of states $\{m^{(i)}(M_z)\}$, for which $\Sigma m^{(i)} = I(M_z)$. The spectrum in this case includes 25 lines, shifts of these lines relative to the central line with the frequency ω_0 are defined by the quantities

$$\Delta(I, I') = I(M_z)B_{\text{eff}}(M_z) - I'(-M_z)B_{\text{eff}}(-M_z) \quad (12)$$

($M_z = 1/2$) and the corresponding intensities are given in table. The general picture for three fours of equivalent ligands is obtained by combination of three above-described spectra.

At first we consider the dipole-dipole contribution to SHFS. For numerical estimates we use the fluorine gyromagnetic ratio $\gamma_I/2\pi = 40\,\text{MHz/T}$ [5] and ligand coordinates $R_1 = 0.222\,\text{nm}$, $\theta_1 = 67.6°$, $R_2 = 0.227\,\text{nm}$, $\theta_2 = 38.6°$ [9, 10], where θ_i are angles between the c-axis and radius-vectors R_i .For thulium nuclei $\gamma_I/2\pi = -3.54\,\text{MHz/T}$, $R_3 = 0.370\,\text{nm}$, $\theta_3 = 44°$. Taking into account given above values of $g_{||}$ and amplification factors $\alpha_{||}$ and $\alpha_\perp$ for thulium nuclear moment, we obtain the following effective fields $\mathbf{B}_d^{(i)} = \gamma_I^{(i)}\mathbf{B}_{\text{eff},d}^{(i)}$ on the ligand's nuclei (components parallel to the c-axis and perpendicular to it are indicated in MHz, $B = 0.55\,\text{T}$):

$$\mathbf{B}_d^{(1)} = (-22 - 2.3M_z, 4.36M_z),$$
$$\mathbf{B}_d^{(2)} = (-22 + 3.20M_z, 5.50M_z),$$
$$\mathbf{B}_d^{(3)} = (5.3 + 0.11M_z, 7.96M_z).$$

Indeed, the dipolar interactions of 5f-electrons of U^{3+} ion with thulium and fluorine nuclei are comparable by value. Note that the dipolar interactions with lithium ions disposed at distances close to those for thulium ions are much less due to the lack of the enhancement of the Li^+ nuclear moments. For this reason lithium nuclei do not contribute to the SHFS of EPR spectra in $LiLuF_4$:U^{3+}, and there is no ground to expect that they will do it in other double fluorides.

The spectra calculated by making use of $\mathbf{B}_d^{(1)}$ and $\mathbf{B}_d^{(2)}$ resemble the experimental spectra for $LiLuF_4$:U^{3+}: they consist of 17 close groups of lines separated by an interval equal approximately to γB, intensities of groups sharply fall with moving away from the center. However, the ratio of the intensities of the neighboring groups ($q/r \approx 1/40$) is much smaller than the experimental one ($\sim 1/4$), that indicates clearly to the importance of the covalence contribution to super-hyperfine interaction. It appeared possible to reach quite satisfactory agreement with experimental data by taking the values of $T_{xz}^{(1,2)}$ and $T_{yz}^{(1,2)}$ greater by 2.5 times than their dipolar values and leaving unchanged the values of $|T_{zz}^{(1,2)}|$. The detailed simulation of the spectrum on the basis of the microscopic model, taking into account the spin transfer from the paramagnetic ion to the ligands, confirmed this simple semi-phenomenological approach [1].

The spectrum obtained by making use of $\mathbf{B}_d^{(3)}$ is far from the experimental one for $LiTmF_4$:U^{3+}. Partly it may be explained by that the Tm^{3+} ion in the vicinity of the doped U^{3+} ion occurs in the distorted crystal field, and its excited doublet $\Gamma_{3,4}$ is split. The first excited level may appear much closer to the ground one, therefore the amplification factor $\alpha_\perp$ becomes greater. The optical spectroscopy data and calculations showed that in the case of the doped Nd^{3+} ion (unfilled $4f^3$ shell) the first excited level of the nearest Tm^{3+} ions has energy of $\sim 20\,\text{cm}^{-1}$ instead of $31\,\text{cm}^{-1}$ in a regular position [11, 12]. For this energy interval, the value of $B_{\perp d}^{(3)}$ is close to 14 MHz. However, the dipolar contribution appears insufficient even with this refinement, and other interactions must be taken into account. For instance, the possibility of exchange interactions was discussed in connection with the spin-lattice

Relative intensities of SHFS lines for four equivalent ligands ($k = r^2 + q^2$)

I/I'	2	1	0	−1	−2
2	r^4	$4r^3q$	$6r^2q^2$	$4rq^3$	q^4
1	$4r^3q$	$4r^2(k+2q^2)$	$12rqk$	$4q^2(k+2r^2)$	$4rq^3$
0	$6r^2q^2$	$12rqk$	$6k^2+12r^2q^2$	$12rqk$	$6r^2q^2$
−1	$4rq^3$	$4q^2(k+2r^2)$	$12rqk$	$4r^2(k+2q^2)$	$4r^3q$
−2	q^4	$4rq^3$	$6r^2q^2$	$4r^3q$	r^4

relaxation in $LiTmF_4$:Nd^{3+} system [11]. Rather well description of the experimental data is obtained if one takes $T_{zz}^{(3)}(1+\alpha_{||}) = 0.1$ MHz (which is close to the dipolar value) and $T_t^{(3)}(1+\alpha_{\perp}) = 60$ MHz (which is about four times larger than the dipolar value). With these figures we have: $\mathbf{B}^{(3)}(M_z) = (5.3+0.1M_z, 60M_z)$, $\varepsilon_{\pm}(M_z = 1/2) = \pm 15.24$, $\varepsilon_{\pm}(M_z = -1/2) = \pm 15.23$ (MHz), $\mathbf{n}_e^{(3)}(1/2)\cdot\mathbf{n}_e^{(3)}(-1/2) = -0.94$, $r^{(3)} = 0.03$, $q^{(3)} = 0.97$. For four thulium ions this brings to five equidistant lines of SHFS separated by 60 MHz and with intensities ratio 1:4:6:4:1, and some lines with much less intensity ($r/q = 1/32$; forbidden transitions). It is just the skeleton of the experimental spectra, the full picture almost coinciding with the experimental spectrum in $LiTmF_4$:U^{3+} at 6 K is obtained by convolution of this skeleton with the fluorine SHFS (similar to the spectrum in Fig.1a). The upper curve *3* in Fig.1b represents the simulated spectrum (the anisotropic exchange interaction $H_{\text{exch}} = -KS_z \sum_i (n_x^i J_{ix} + n_y^i J_{iy}) n_z^i$ between U^{3+} and Tm^{3+} ions with the exchange constant $K = 4.2$ GHz was considered to account for the enhanced coupling between the $5f$ electrons and thulium nuclei through thulium $4f$ electrons with the total angular moments $\mathbf{J}_i$; line shapes of individual transitions were assumed to be Gaussians with a half-width of 2 MHz). The temperature transformation of the spectrum is qualitatively explained by the temperature dependence of the amplification factor $\alpha_{\perp}$ (see [13]). This factor is decreased by 20% in the temperature interval $5 \div 15$ K in the regular crystal. The decrease of the separation between main peaks in the observed SHFS of the $LiTmF_4$:U^{3+} spectrum is larger due to the discussed above distortion of the crystal field on thulium ions in the nearest surroundings of impurity U^{3+} ions.

Thus the main features of the complex EPR spectra of U^{3+} ions introduced in the $LiTmF_4$ crystals are explained within the existing theories of SHFS of EPR spectra and of Van Vleck paramagnetism.

This work was supported by Ministry of Science and Education of Russian Federation (project RNP 2.1.1.7348) and Federal center for physical and chemical measurements.

1. L. K. Aminov, A. A. Ershova, D. G. Zverev et al., Applied Magnetic Resonance **33**, (2007) [doi:10.1007/s00723-007-0000-0].
2. L. K. Aminov, B. Z. Malkin, and M. A. Teplov, in *Handbook on the Physics and Chemistry of Rare Earths*, vol. 22, Ed. K. A. Gschneidner, Jr. and L. Eyring, Elsevier Science, 1996, p. 295.
3. H. P. Jenssen, M. A. Noginov, and A. Cassanho, OSA Proc. Adv. Solid-State Lasers **15**, 463 (1993).
4. J. E. Miller and E. I. Sharp, J. Appl. Phys. **41**, 4718 (1970).
5. A. Abragam and B. Bleaney, *Electron Paramagnetic Resonance of Transition Ions*, Clarendon, Oxford, 1970.
6. U. Ranon and J. S. Hyde, Phys. Rev. **141**, 259 (1966).
7. B. R. Mc Garvey, J. Chem. Phys. **20**, 837 (1976).
8. R. M. Macfarlane, R. S. Meltzer, and B. Z. Malkin, Phys. Rev. B **58**, 5692 (1998).
9. E. Garcia and R. P. Ryan, Acta Cryst. C **49**, 2053 (1993).
10. A. Bensalah, Y. Guyot, A. Brenier et al., J. Alloys Compd. **380**, 15 (2004).
11. L. K. Aminov, A. V. Vinokurov, I. N. Kurkin et al., Phys. Status Solidi (b) **152**, 191 (1989).
12. L. K. Aminov, B. Z. Malkin, M. A. Koreiba et al., Optika i Spektroskopiya **68**, 835 (1990).
13. I. S. Konov and M. A. Teplov, Fiz. Tverd. Tela (Leningrad) **18**, 1114 (1976).